

PAPER • OPEN ACCESS

## Evaluation of induced activity in various components of a PET-cyclotron

To cite this article: A. Toyoda *et al* 2018 *J. Phys.: Conf. Ser.* **1046** 012017

View the [article online](#) for updates and enhancements.

### You may also like

- [Research on the effect of the external magnetic field in the joule balance at NIM](#)  
Jinxin Xu, Qiang You, Zhengkun Li et al.
- [A magnet system for the MSL watt balance](#)  
C M Sutton and M T Clarkson
- [Two simple modifications to improve the magnetic field profile in radial magnetic systems](#)  
Shisong Li and Stephan Schlamminger



**ECS**  
The  
Electrochemical  
Society  
Advancing solid state &  
electrochemical science & technology

**DISCOVER**  
how sustainability  
intersects with  
electrochemistry & solid  
state science research

# Evaluation of induced activity in various components of a PET-cyclotron

A. Toyoda<sup>1</sup>, G. Yoshida<sup>1</sup>, H. Matsumura<sup>1</sup>, K. Masumoto<sup>1</sup>, T. Nakabayashi<sup>2</sup>, T. Yagishita<sup>2</sup> and H. Sasaki<sup>2</sup>

<sup>1</sup>Radiation Science Centre, High Energy Accelerator Research Organization (KEK), Oho Tsukuba, Ibaraki, Japan

<sup>2</sup>Japan Environmental Research Co., Ltd., 1-24-6 Nishi-Shinjuku, Shinjuku, Tokyo, Japan

akihiro.toyoda@kek.jp

**Abstract.** For decommissioning a cyclotron facility, it is important to evaluate the induced activity of the various components of the cyclotron; however, activation of the metal components has been rarely investigated. In this study, two types of cyclotrons were examined; one is a proton acceleration type using a deflector, and another is a hydride ion (H<sup>-</sup>) acceleration type using a carbon stripper foil for beam extraction to the target port. The samples were obtained from various metal components such as the yoke, sector magnet, coil, and vacuum chamber by the core boring method, and the depth distribution of the radioactivity was determined via a germanium semiconductor detector. The activities of <sup>54</sup>Mn and <sup>60</sup>Co were detected from the surface to a deeper site of the yoke and sector magnet. Most of the observed activities of the cyclotron components were higher than the clearance levels, suggesting that a clearance system should not be applied to the yoke and sector magnet. In the case of a high-activity sample, we have to wait for 30 years to reach the clearance level.

## 1. Introduction

In Japan, various small-scale cyclotron facilities had been established for the generation of radiopharmaceuticals for use in positron emission tomography (PET). However, some facilities are aging, and it is expected that the number of systems to be decommissioned will drastically increase in the future. Though radioactive waste generation during the decommissioning of a cyclotron must be strictly controlled, extremely low-level radioactive wastes cannot be regarded as radioactive. Thus, such wastes can be treated as ordinal materials in a clearance system in Japan [1], and borderlines are configured for each nuclide (clearance level) [2]. For progressing the decommissioning of a cyclotron efficiently, a clearance system should be extensively utilized and the amount of radioactive waste generation should be reduced. Therefore, the methods to evaluate the activation of the components and facilities and to analyse samples must be clarified for the various types of cyclotron facilities.

In this regard, we examined the activation of two types of cyclotrons; one is a proton acceleration type using a deflector, and the other is a hydride ion (H<sup>-</sup>) acceleration type using a carbon stripper foil for beam extraction to the target port. In both types, radionuclides get accumulated in the metal components during operation (i.e., radiopharmaceutical generation). It is already known that <sup>60</sup>Co and



$^{54}\text{Mn}$  are generated in the metal components of a cyclotron, such as the yoke, sector magnet, vacuum chamber, and coil [3]; however, their radioactivity and distribution have not been comprehended yet. In this study, we examined the radionuclides that were induced in the metal components of a cyclotron and determined the depth and area distribution to obtain the fundamental data for conducting decommissioning.

## 2. Experimental procedures

### 2.1. Cyclotrons for sampling

The specifications of the two types of cyclotrons that were examined in this study are summarized in Table 1, and their diagrammatic outlines are shown in Figure 1. BC1710 that is manufactured by Japan Steel Works (JSW) is a proton acceleration type cyclotron and is not self-shielded. It was installed in a public hospital in the Kyoto prefecture, and was used from 2003 to 2016 for a total operation time of 3400 h. The principal parts of this cyclotron and its materials are as follows: yoke (iron), vacuum chamber (stainless steel), and coil (copper). We took samples from this cyclotron on 25 July 2016.

CYCLONE 10/5 that is manufactured by Ion Beam Applications (IBA) Belgium is a  $\text{H}^-$  acceleration type cyclotron with self-shielding. This type accelerates hydride ions and strips all the electrons using a carbon foil just before injection into a target. It was installed in a university hospital in the Mie prefecture, and was used from 2003 to 2011 for a total operation time of approximately 2600 h. The principal parts of this cyclotron and their materials are as follows: yoke (iron), sector magnet (iron), coil (copper), and vacuum chamber (aluminium). We took samples from this cyclotron on 24 May 2016. Both models were mainly used to produce  $^{18}\text{F}$  as a radiopharmaceutical for PET.

**Table 1.** Specifications of the cyclotrons

	BC1710	CYCLONE 10/5
Manufacturer (Country)	JSW (Japan)	IBA (Belgium)
Self-shield material	None	Concrete
Maximum energy	17 MeV (p), 10 MeV (d)	10 MeV ( $\text{H}^-$ ), 5 MeV ( $\text{D}^-$ )
Maximum current	50 $\mu\text{A}$ (p), 50 $\mu\text{A}$ (d)	60 $\mu\text{A}$ ( $\text{H}^-$ ), 35 $\mu\text{A}$ ( $\text{D}^-$ )
Operation time	4/2003–4/2016	3/2003–11/2011
Total operation time	3400 [h]	2598 [h]
Sampling date	25/7/2016	24/5/2016

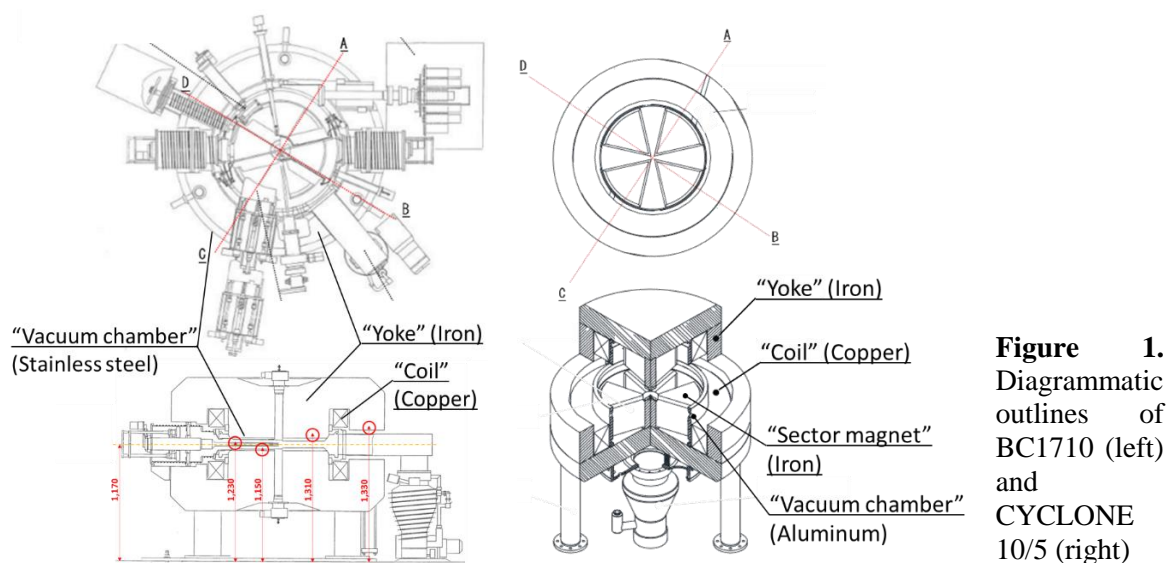


**Figure 1.** Diagrammatic outlines of BC1710 (left) and CYCLONE 10/5 (right)

## 2.2. Core boring and sample preparation

Sample preparation processes are shown in Figure 2. Both the cyclotrons were divided into individual components, and core samples were extracted from the yoke, sector magnet, coil, and vacuum chamber by a drill (core boring method [4,5]). First, to easily assess the activation level of each part, the surface dose rate of the core samples was measured via a sodium iodide (NaI) scintillation survey meter (TCS-161, Hitachi). The measurements were performed along the axial direction in steps of 5 cm from the surface. We adopted the median of each unit as the measuring point (i.e. 2.5 cm, 7.5 cm, 12.5 cm...). The time constant of the survey meter was 10 s. After the dose rate measurement, the samples were sliced into 1-cm test pieces. Each test piece was packed in a plastic container (U8 type) and characterized by  $\gamma$ -ray spectrometry. Such core sampling from the metal components of a small-scale medical purpose cyclotron and similar activity measurements have been rarely performed.



**Figure 2.** Principal processes of sample preparation, a) core samples (diameter: 5 cm, length 3–36 cm) were extracted from the metal components of the cyclotron using a core drill, b) extracted samples were sliced into 1-cm-thick test pieces by a tip saw after the dose rate measurement via a sodium iodide (NaI) scintillation survey meter, and c) each test piece was packed in a plastic container (U8 type) for characterization by  $\gamma$ -ray spectrometry.

## 2.3. $\gamma$ -ray spectrometry

We performed  $\gamma$ -ray spectrometry, using a germanium semiconductor detector (GMX-20195-S, ORTEC), for the test pieces prepared by the method described in the previous sub-section. The detector head was shielded by an inner sleeve (5 mm of copper and 5 mm of acrylic) and an outer sleeve (11 cm of lead and 5 cm of iron). The measurement time was 10000 s for each sample. The detection efficiency was determined using the standard radioisotopes (RI) solution of the Japan

Radioisotope Association (JRIA). Simultaneously, the self-absorption by the sample and sum-peaks were corrected. The activity of each nuclide was corrected on the sampling date.

### 3. Results and discussion

#### 3.1. Dose rate of a core sample at each sampling point

The dose rates of the core samples are summarized in Tables 2 and 3. The background of the measurement is 0.06  $\mu\text{Sv/h}$ , and the detection limit is 0.09  $\mu\text{Sv/h}$ . The values presented in the tables include the background. From the results of BC1710, we find that the dose rates of the yoke (Nos.1–10 in Table 2) are much higher than the background level at all the sampling points until a depth of 20 cm. In contrast, for CYCLONE (Table 3), the dose rates are almost similar to the background level at numerous sampling points. It was expected for the short-lived nuclides to have decayed because 4.5 years had elapsed since the end of operation. The dose rates of the vacuum chamber of BC1710 (Nos.11–13 in Table 2) were quite high because of the presence of short-lived nuclides such as  $^{51}\text{Cr}$ ,  $^{57}\text{Co}$ , and  $^{58}\text{Co}$  that were generated by nuclear reactions with Cr and Ni. These three samples were only 3.3 cm in length, and thus, a median length of 1.65 cm was adopted as the measurement point.

**Table 2.** Dose rates of the core samples extracted from BC1710 ( $\mu\text{Sv/h}$ )

Sample name	Depth from the surface					
	2.5 cm	7.5 cm	12.5 cm	17.5 cm	22.5 cm	27.5 cm
Yoke (Nos.1–10)						
No.1	0.21	0.19	0.14	0.11	0.09	0.08
No.2	0.31	0.35	0.29	0.20	0.14	0.11
No.3	0.19	0.17	0.14	0.12	0.11	0.10
No.4	0.33	0.28	0.21	0.14	0.12	0.10
No.5	0.22	0.19	0.14	0.11	0.10	0.08
No.6	0.23	0.22	0.16	0.12	0.10	0.09
No.7	0.40	0.35	0.23	0.15	0.10	
No.8	0.23	0.23	0.18	0.15	0.12	0.09
No.9	0.36	0.31	0.23	0.16	0.11	0.10
No.10	0.21	0.20	0.15	0.12	0.10	0.08
Depth from the surface						
1.65 cm						
Vacuum chamber (Nos.11–13)						
No.11	1.40					
No.12	2.40					
No.13	1.05					

**Table 3.** Dose rates of the core samples extracted from CYCLONE 10/5 ( $\mu\text{Sv/h}$ )

Sample name	Depth from the surface					
	2.5 cm	7.5 cm	12.5 cm	17.5 cm	22.5 cm	27.5 cm
Sector magnet (Nos. 1-8):						
No.1	0.21	0.22	0.20	0.19	0.17	0.13
No.2	0.06	0.06	0.06	0.06	0.06	0.06
No.3	0.09	0.10	0.09	0.08	0.08	0.07
No.4	0.09	0.09	0.09	0.09	0.08	0.07
No.5	0.17	0.18	0.17	0.16	0.14	0.12
No.6	0.06	0.06	0.06	0.06	0.06	0.06
No.7	0.09	0.10	0.10	0.10	0.09	0.08
No.8	0.08	0.09	0.09	0.09	0.09	0.07
Yoke (Nos. 9-24):						
No.9	0.06	0.06	0.06	0.06		
No.10	0.06	0.06	0.06	0.06		
No.11	0.11	0.10	0.08	0.07		
No.12	0.06	0.06	0.06	0.06		
No.13	0.06	0.06	0.06	0.06		
No.14	0.11	0.10	0.08	0.06		
No.15	0.06	0.06	0.06	0.06		
No.16	0.06	0.06	0.06	0.06		
No.17	0.06	0.06	0.06			
No.18	0.22	0.18	0.11			
No.19	0.07	0.06	0.06			
No.20	0.06	0.06	0.06			
No.21	0.06	0.06	0.06			
No.22	0.06	0.06	0.06			
No.23	0.25	0.21	0.13			
No.24	0.06	0.06	0.06			
Coil (Nos.25-32):						
No.25	0.08	0.06	0.06	0.06		
No.26	0.06	0.06	0.06	0.06		
No.27	0.06					
No.28	0.06					
No.29	0.08					
No.30	0.06					
No.31	0.06					
No.32	0.06					

### 3.2. Depth distribution of the nuclides induced in the cyclotron metal components

From the results of the dose rate measurements recorded by the survey meter, it was revealed that radioactivity was induced in the deep sites of the components. In this section, we discuss the  $\gamma$ -ray spectrometry that was performed for the test pieces (sliced core samples) to investigate the type of nuclides generated in the cyclotron. The lengths of the yoke and sector magnet being suitable to determine the depth distribution of the nuclides and the corresponding samples were chosen for the spectrometry measurements. The sampling points for the yoke of BC1710 and depth distribution of the nuclides at each point are shown in Figure 3. The bottom side of the yoke is depicted as the area shaded in blue in Figure 3. The sample cores were extracted along the red lines directed from the centre to the outside. The horizontal axis denotes the core sample depth, from the centre to the outside direction. The vertical axis corresponds to the specific activity of a particular nuclide at each depth. As shown in Figure 3,  $^{54}\text{Mn}$  (green diamond) and  $^{60}\text{Co}$  (red triangle) are detected at all the sampling points. Although in a small amount,  $^{59}\text{Fe}$  (yellow circle) is also detected. The specific activity of  $^{54}\text{Mn}$  rapidly decreases with the depth, whereas that of  $^{60}\text{Co}$  decreases relatively slowly.  $^{54}\text{Mn}$  was generated by the fast neutron, whereas  $^{60}\text{Co}$  was mainly generated by the thermal neutrons. Such differences in the production process could influence the activity at each depth. At sampling points Nos. 6–8 and 10, the specific activity of  $^{60}\text{Co}$  decreases with the depth, though there is a slight increase at the end point of the core sample. This is caused by the reflected neutrons generated by the shield wall which is just outside the yoke.

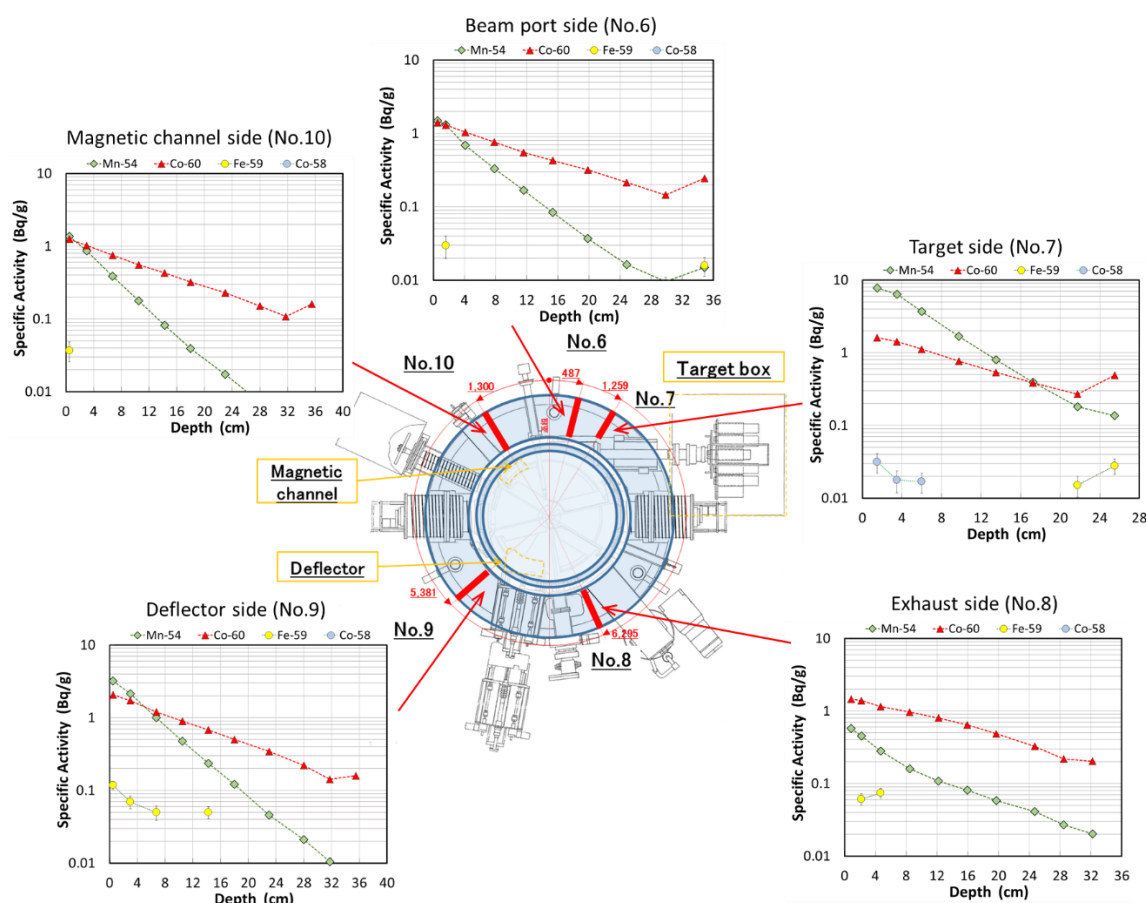


**Figure 3.** Depth distribution of the specific activity of the principal nuclides at the sampling points (BC1710, bottom side of the yoke). The yoke is the area shaded in blue. The sample cores were extracted along the bold red lines directed from the centre to the outside.

The sampling points for the yoke of CYCLONE 10/5 and depth distribution of the nuclides at each point are shown in Figure 4. The second stage of the yoke is depicted as the area shaded in blue in Figure 4, whereas the red lines depict the sample cores. In all the sampling points shown in Figure 4,  $^{60}\text{Co}$  is detected, whereas  $^{54}\text{Mn}$  is mainly detected in the target side (No.23). Similar to BC1710, the specific activity of  $^{54}\text{Mn}$  rapidly decreases with depth, whereas that of  $^{60}\text{Co}$  decreases more slowly. The activity levels of  $^{54}\text{Mn}$  and  $^{60}\text{Co}$  are similar to those of the yoke of BC1710 at the point close to the target (No.23 of CYCLONE and No.7 of BC1710). In comparison, in the other areas, the activity levels are much lower than those of BC1710, even when considering the attenuation of the activity by a time-lapse. This result reflects that the beam loss in the H<sup>-</sup> acceleration type cyclotron is much smaller than in the proton acceleration type.

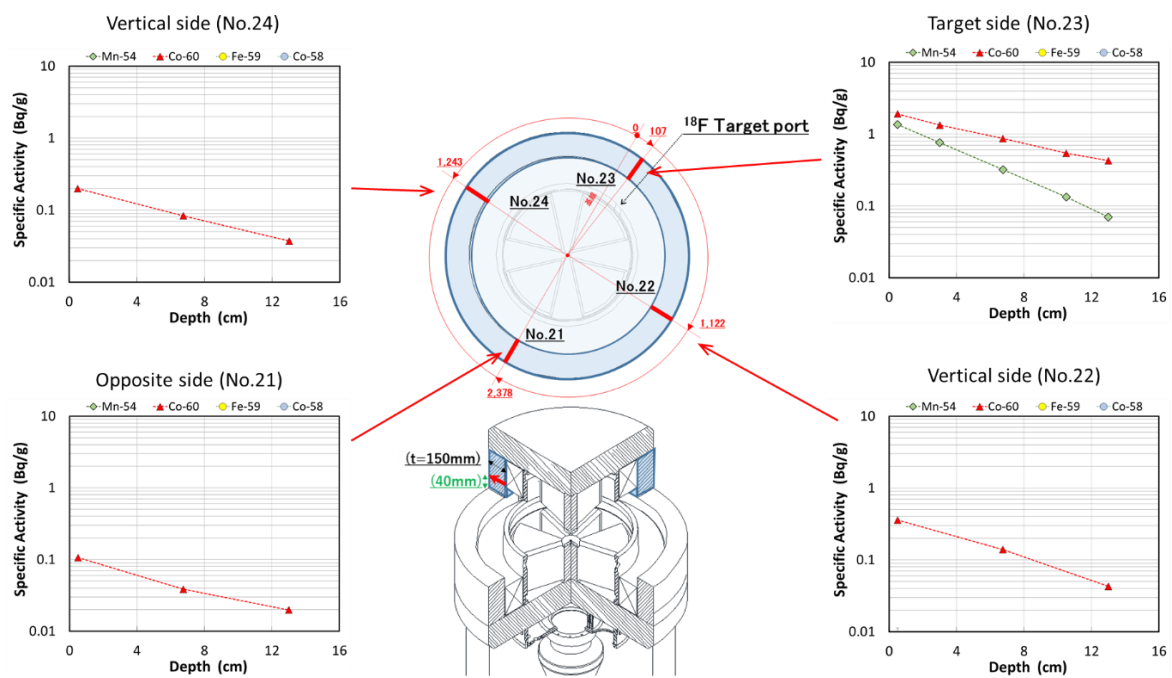


**Figure 4.** Depth distribution of the specific activity of the principal nuclides at the sampling points (CYCLONE 10/5, Second stage of Yoke). The yoke is the area shaded in blue. The sample cores were extracted along the bold red line from the centre to the outside direction.

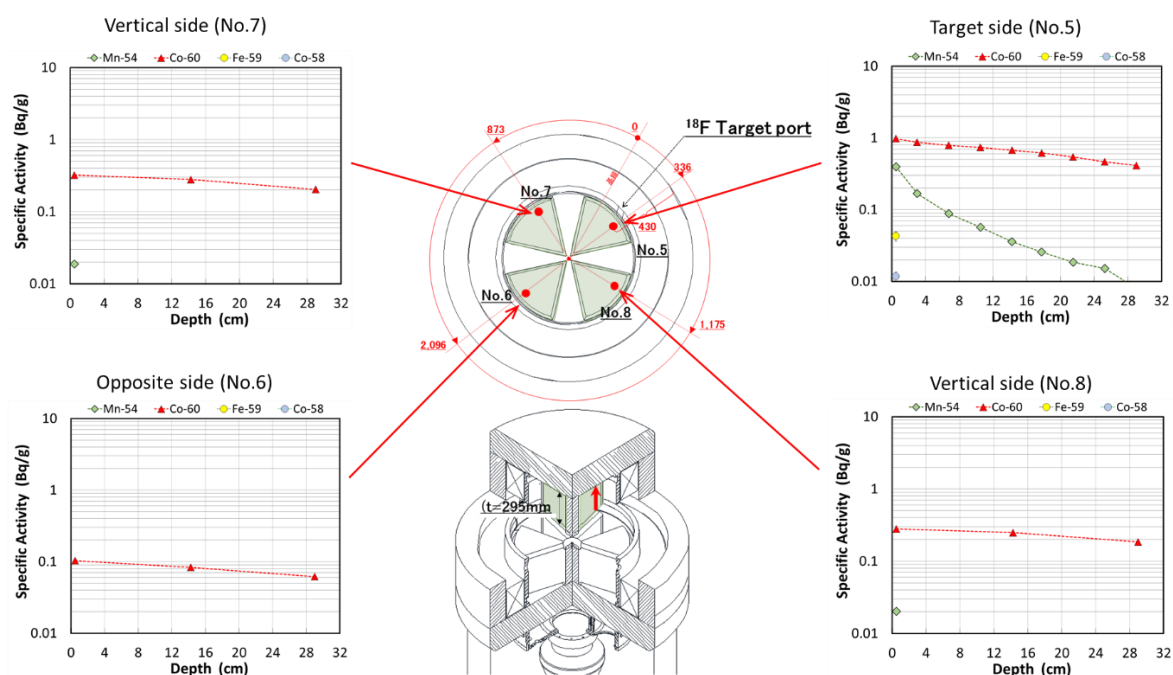


**Figure 5.** Depth distribution of the specific activity of the principal nuclides at the sampling points (CYCLONE 10/5, top side of the sector magnet). The sector magnet is the area shaded in green. The sample cores were extracted from the direction of the bottom to the top at each red dot.

The sampling points of the sector magnet in CYCLONE 10/5 and depth distribution of the nuclides at each point are shown in Figure 5. The sector magnet is the area shaded area in Figure 5. Same as the results for the yoke,  $^{60}\text{Co}$  is detected at all the sampling points in Figure 5, and  $^{54}\text{Mn}$  is mainly detected on the target side (No.5). The specific activity of  $^{54}\text{Mn}$  rapidly decreases with the depth. This is the same trend as for the yoke. As a unique trend of the sector magnet, the specific activity of  $^{60}\text{Co}$  only slightly decreases with the sample depth. It is implied that the thermal neutrons were distributed in the entire body of the sector magnet during the operation. The activity level of  $^{60}\text{Co}$  is almost same to that of the yoke in CYCLONE 10/5, whereas the level of  $^{54}\text{Mn}$  is lower.

### 3.3. Verification of the activity of the cyclotron components by the clearance level

The ratio of the observed activity to the clearance level (D/C) was considered for the results presented in section 3.2. The clearance level of both  $^{54}\text{Mn}$  and  $^{60}\text{Co}$  is 0.1 Bq/g, and the specific activity of the components must be below the clearance level to treat the radioactive wastes as normal wastes (i.e.,  $D/C < 1$ ). In the case of BC1710 (Figure 3), D/C is larger than 1 at all the sampling points and depths. Furthermore, in case of CYCLONE 10/5 (Figures 4 and 5), D/C is larger than 1 at various sampling points. The D/C ratio is marginally lower than 1 at only two sampling points (Nos. 6 and 21). In the case of the highest activity sample, it is expected that 30 years or more will be necessary to reduce the activity level below the clearance level. From these facts, it is found that the cyclotron main components (yoke and sector magnet) cannot be treated as normal wastes, regardless of the acceleration particles. These must be controlled as radioactive wastes.

## 4. Conclusions

We analysed the core samples from two types of small-scale medical purpose cyclotrons. We examined the radioactivity of the nuclides generated in the metal components of the cyclotrons and determined the depth distribution. In all the samples,  $^{54}\text{Mn}$  and  $^{60}\text{Co}$  were detected as the principal nuclides.  $^{54}\text{Mn}$ , which was generated by the fast neutron reactions, was mainly detected close to the

target port and rapidly decreased with the depth. In contrast,  $^{60}\text{Co}$ , which was generated by the thermal neutrons in all the parts, slowly decreased with depth. The difference, which was attributed to the acceleration particles, was very small. The metal components of the cyclotron such as the yoke and sector magnet should be treated as radioactive wastes because their activity is expected to be much higher than the clearance level.

### References

- [1] <https://www.nsr.go.jp/activity/regulation/nuclearfuel/haiki4.html> (Japanese only)
- [2] Okoshi M 2002 *Jpn. J. Health Phy.* **37**(3) pp197–207
- [3] Ito K, Nakata Y, Matsuda H, and Sato N 2011 *Kaku Igaku.* **48**(2) pp109–119
- [4] Saito K, Takahashi Y, Yamaguchi I, Kimura K, Kanzaki T, Shimada H, Otake H, Oriuchi N, and Endo K 2009 *Jpn. J. Med. Phys.* **29**(2) pp29–34
- [5] Masumoto K, Ohtsuki T, Kasagi J, Izumi Y, and Yamato I 1999 *Jpn. J. Health Phy.* **34**(2) pp151–160